








The histology and growth rate of Nile crocodile (*Crocodylus niloticus*) claws

Albert Myburgh^{1,2}  | Jan Myburgh²  | Johan Steyl²  | Colleen T. Downs¹  | Hannes Botha^{3,4}  | Liam Robinson⁵  | Stephan Woodborne⁶ 

¹Centre for Functional Biodiversity, School of Life Sciences, University of KwaZulu-Natal, Pietermaritzburg, South Africa

²Department of Paraclinical Sciences, Faculty of Veterinary Science, University of Pretoria, Pretoria, South Africa

³Scientific Services, Mpumalanga Tourism and Parks Agency, Nelspruit, South Africa

⁴Department of Biodiversity, University of Limpopo, Polokwane, Limpopo, South Africa

⁵Department of Oral and Maxillofacial Pathology, School of Dentistry, Oral Pathology and Oral Biology Department, University of Pretoria, Pretoria, South Africa

⁶iThemba LABS, Cape Town, South Africa

Correspondence

Albert Myburgh, Centre for Functional Biodiversity, School of Life Sciences, University of KwaZulu-Natal, Private Bag X01, Scottsville, Pietermaritzburg 3209, South Africa.

Email: Albert.Myburgh@up.ac.za

Funding information

Idea Wild; National Research Foundation South Africa

Abstract

The histology and growth of reptilian and crocodylian claws (ungues) have been extensively studied; however, Nile crocodile (*Crocodylus niloticus*) claws have not received adequate attention. Furthermore, age estimations for reptilian claws remain unexplored, despite Nile crocodile claws being used in long-term dietary reconstruction studies, assuming certain age-related patterns. In this study, we investigate the histology and growth patterns of Nile crocodile claws, aiming to infer axes for sampling cornified material for radiocarbon dating and establish age estimations for crocodylian claws. Our findings reveal that Nile crocodile claws exhibit growth patterns similar to other reptilians, presenting as modified scutes/scales with an age profile along the sagittal plane. This profile starts at the basal germ matrix and progressively expands in thickness and age dorsoventrally towards the apex or “tip.” Consequently, the oldest corneous material is concentrated at the most dorsal point of the claw's apex. To validate previous dietary reconstruction assumptions, we conducted radiocarbon dating on this region of the claw, which supported the idea that retained corneous material in the claws is typically relatively young (5–10 years old) due to abrasion. Our study contributes insights into the histology and growth dynamics of Nile crocodile claws, shedding light on their use in dietary reconstruction studies and emphasizing the significance of considering age-related assumptions in such investigations.

KEYWORDS

age estimation, dietary reconstruction, growth patterns, radiocarbon dating, reptilian claw

1 | INTRODUCTION

Ecologists use variations in naturally occurring isotopes to reveal dietary relationships among organisms (Boecklen et al., 2011; Layman et al., 2012), patterns of migration (Barquete et al., 2013; Cerling et al., 2006; Hobson & Wassenaar, 2018), and to investigate ecological

change (Dawson & Siegwolf, 2007). Shifts in food web dynamics (the relative trophic position of organisms in a food web) have become important indicators of ecosystem state, especially in aquatic systems (Krause et al., 2019; Vander Zanden et al., 1999; Wang et al., 2014;). Isotope analysis of temporally resolved tissues, such as claws, baleen, feathers and hair that grow ubiquitously while remaining inert after

This is an open access article under the terms of the Creative Commons Attribution-NonCommercial-NoDerivs License, which permits use and distribution in any medium, provided the original work is properly cited, the use is non-commercial and no modifications or adaptations are made.

© 2023 The Authors. *Journal of Morphology* published by Wiley Periodicals LLC.

their formation, is particularly useful because it can be used to resolve temporal changes in dietary assimilation (Dalerum & Angerbjörn, 2005). It reveals trophic relationships as well as migration data that is otherwise difficult to determine using conventional observations (Hobson & Wassenaar, 2018; Layman et al., 2012).

The chemical composition, as well as a detailed description of the development and structure of various reptilian claws, appear elsewhere (Alibardi, 2021; Chang et al., 2009); however, notable differences exist during reptilian claw development between different taxa. In crocodylians, the cornification process differs from that of other taxa by the region of cell proliferation and growth, which is not localized in a nail groove, but dividing cells are equally distributed along the epidermis on the last phalange from the base, proximally, to the tip, distally (Alibardi, 1998, 2016; Alibardi & Thompson, 2002; Maderson & Alibardi, 2000; Rutland et al., 2019). Claws appear as modified scales/scutes, where growth patterns are retained, and cornification occurs along the length/sagittal plane of the claw (Alibardi, 2010, 2016; Alibardi & Thompson, 2002) as the cytoplasmic content of epidermal cells is replaced by filamentous proteins (Alibardi, 2021; Tomlinson et al., 2004). The result is a transformation from living, functional cells to cornified structurally dead and chemically inert cells (Ethier et al., 2013; Mülling, 2000; Wang et al., 2016). The histology of reptilian and crocodylian claws, in particular, has been investigated (Alibardi, 2009, 2010, 2021), but the histology of the claws of the Nile crocodile has not been reported, and age estimations of the cornified structures of crocodylian claws have not been attempted.

Radiocarbon dating provides age measurements of carbon-based materials with biological origins (Bowman, 1990; Hajdas et al., 2021). Advances in the last three decades have helped produce measurements with greater accuracy on smaller samples (typically in the mg range), allowing researchers in a number of disciplines to address chronological questions that could not be dealt with 10 or 20 years ago (Bronk Ramsey, 2008; Hajdas et al., 2021). Human hair was one of the first samples to be dated using the technique (Libby, 1954; Nardoto et al., 2020). An important factor in applying radiocarbon dating to resolve biological growth patterns on living organisms is the effect of large-scale above-ground nuclear bomb testing in the mid-20th century. This affected atmospheric ^{14}C concentrations (known as the bomb curve) that is entirely distinct from ^{14}C concentrations before 1950 CE (Dutta, 2016; Hodge et al., 2011; Reimer et al., 2004), and tissue grown in the last 70 years will contain "bomb carbon." Since the rise and subsequent decline in the bomb carbon curve is well quantified, radiocarbon analysis can be used to resolve ages with an annual or intra-annual resolution for tissue formed in the last 70 years. The approach is a novel way of estimating the date of tissue formation, and accordingly the age and growth rates. Cornified tissue such as claw keratin is considered appropriate material for radiocarbon dating (Hajdas et al., 2021).

The distribution of the growth layers in the claws of crocodylians and other reptiles should yield a distinct age profile across the dorsal-sagittal axis of the claw. A time series of this nature is potentially useful in growth rate or age determination, but it could be used in combination with stable isotopes or trace element analysis to investigate dietary histories or migrations. This was implied but not tested in the study of

diet histories of Nile crocodiles in the Kruger National Park, South Africa, following a pansteatitis epidemic (Woodborne et al., 2012). Pansteatitis is a dietary disease associated with the discoloration and hardening of fat (Huchzermeyer, 2002). The disease caused a drastic decline in the Nile crocodile population of the Olifants river gorge in the Kruger National Park between 2008 and 2011 (Ferreira & Pienaar, 2011; Huchzermeyer, 2012; Myburgh & Botha, 2009).

Stable isotope analyses showed dietary aetiology to pansteatitis associated with nutrient pollution as filter-feeding fish in the Olifants River Gorge had elevated $\delta^{15}\text{N}$ values linked to pollutant driven algal blooms (Woodborne et al., 2012). Samples along the basal-distal axis of the unguis of Nile crocodile claws from postmortem animals had patterned cycles in $\delta^{15}\text{N}$ attributed to episodic fish binge feeding, and it was proposed that this exposure pathway (to pollutants) was the cause of the mass mortalities (Woodborne et al., 2012). These periodic elevations in $\delta^{15}\text{N}$ were assigned a nominal time axis in the absence of data on the growth and wear rates of Nile crocodile claws and lacked the time scale needed to link the disease outbreak to chronological changes in river morphology and nutrient/pollutant dynamics. Further investigation into the development and age of crocodylian claws were suggested as this would constrain the uncertainties around the temporal scales of this fish binge feeding hypothesis (Woodborne et al., 2012). In this study, we investigated the histology of the claw of the Nile crocodile and used the structure to inform the sampling of cornified material for radiocarbon dating to estimate the retention time of cornified material along the claw. We hypothesized that the claws of Nile crocodiles retain corneous material for relatively short periods of time (10 years or less) and that the patterned spikes of $\delta^{15}\text{N}$ observed by Woodborne et al. (2012) are annual spikes associated with fish binge feeding. Alternatively, whether the claws of Nile crocodiles are older than 20+ years can be tested using the radiocarbon associated with above-ground nuclear testing. If this is the case, then the $\delta^{15}\text{N}$ patterns of Woodborne et al. (2012) are not annual, and the fish binge feeding hypothesis is rejected.

2 | MATERIALS AND METHODS

2.1 | Histology

Limbs from hatchling Nile crocodiles ($n = 3$ claws from 3 different animals) *Crocodylus niloticus* (Laurenti 1768) were obtained from natural mortalities at a crocodile farm through collaboration with the Exotic Leather Research Centre, Faculty of Veterinary Science, University of Pretoria (UP), Pretoria, South Africa, under ethical clearance from the University of KwaZulu-Natal, protocol reference number 020/15/Animal.

All histological processing and examinations were conducted at the Section of Pathology, Faculty of Veterinary Science, UP, during 2021. Limbs were fixed in 10% buffered formalin for at least 48 h postsampling. Sub-samples containing phalanges and claws were sectioned and trimmed in the sagittal and transverse plane before being routinely processed for hematoxylin & eosin staining and light microscopic histological examination (Bancroft & Gamble, 2002).

Corneal layers of claws collected from one wild and one captive adult crocodile were obtained from postmortem examinations. These crocodile claws were embedded using EpoFix Resin, a cold mounting media that supports the sample during sectioning. This enables easy handling and clamping of the sample to ensure uniform sectioning. The embedded claw samples were sectioned using a Secotom Precision Cutting Machine (Struers S.A.S., France) to produce 240–260 μm cross sections. After cutting was completed, all sections were washed in running tap water to remove surface debris, followed by ultrasonic cleaning to remove any residual debris.

The sections were then stained using a Warthin-Starry histochemical stain according to standard procedures. Sections were impregnated with a silver solution followed by a developer solution consisting of hydroquinone, gelatine and silver. The sections were then toned in a 2% gold chloride solution and the color fixed using 5% sodium thiosulphate. Finally, the sections were rinsed in distilled water, dehydrated and placed on a glass slide for microscopic evaluation (Bancroft & Gamble, 2002).

2.2 | Radiocarbon dating

One claw each (largest claw on the back foot) from two wild Nile crocodile individuals ($\pm 3\text{ m}$ total length [TL]) were obtained from carcasses found during aerial surveys of the Olifants River in the Kruger National Park, South Africa, and another claw was obtained from a postmortem investigation of a large crocodile (5.05 m TL) in the middle regions of the Olifants River, under permit number MPB 9225/2 from the Mpumalanga Tourism and Parks Agency. Claws were removed from animals several days following their death. The Kruger National Park Nile crocodiles succumbed to unknown circumstances whilst the larger individual starved to death after it had swallowed fishing nets. Claws were removed by severing the phalanges with the largest claws from the back foot of the animal using a scalpel. The non-hatchling crocodiles included in this study were of an unknown age as they were either wild caught with no record of birth and growth rates, or they were wild caught and housed on crocodile farms for >30 years with no record of birth dates.

Claw preparation and radiocarbon dating was conducted at iThemba LABS, Johannesburg, South Africa. Soft tissue and cornified material were separated by boiling claws in distilled water for approximately 3 h. Thereafter, claws were cleaned with a sterile toothbrush and sectioned, dorsoventrally in half, using a diamond-edged cutting blade on a Dremel™ rotary tool. A photograph of the sectioned claw was taken under a dissection microscope, imported and outlined in Designspark (Designspark Mechanical 5.0 [ANSYS Inc. 2020]) for graphical representation.

From the Kruger National Park Nile crocodile claws, four samples were obtained from the unguis of the claw following the methods of Woodborne et al. (2012). The claw from the larger crocodile was sampled similar to the others, but an additional sample set was obtained along the basal dorsal axis of the claw through the unguis at the claw tip. For this claw, both sampling directions included a common sample (asterisk in Figure 1), for a total of seven radiocarbon samples from a single claw. Samples of $\pm 6\text{ mg}$ were obtained at the selected locations using a dental drill (Figure 1). Four additional samples were obtained from living animals in the Olifants River, Kruger National Park, by scraping cornified material from the claw tip (asterisk in Figure 1) during routine health assessments on captured Nile crocodiles in the Kruger National Park.

The radiocarbon measurements were conducted at the AMS Facility of iThemba LABS, Johannesburg, Gauteng, South Africa, using the 6 MV Tandem AMS system (Mbele et al., 2017). The radiocarbon dates and errors were rounded to the nearest year. Radiocarbon dates were calibrated and converted into calendar ages with the OxCal v4.4 for Windows by using the SHCal20 atmospheric data set (Hogg et al., 2020).

3 | RESULTS

3.1 | Histology

The claw of the Nile crocodile is similar in structure to that of the American alligator (*Alligator mississippiensis*) described in Alibardi (2009, 2021) and Alibardi and Thompson (2002) (Figure 2). Corneocytes

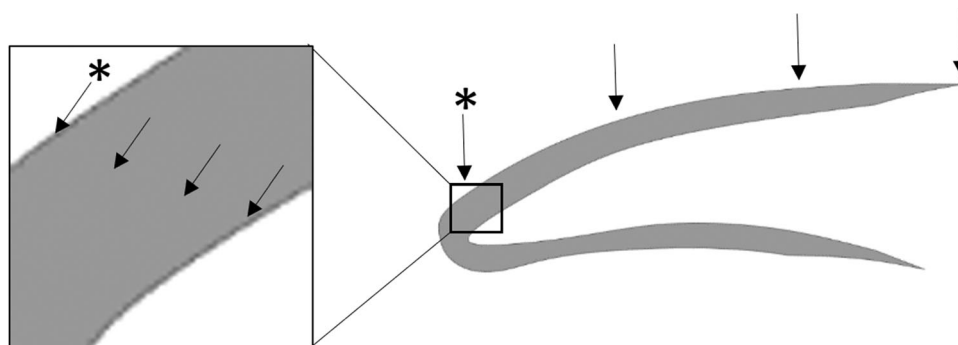


FIGURE 1 Sampling locations for radiocarbon dating along Nile crocodile claws in the present study. Arrows indicate sample locations, and those marked with an asterisk are from the same location. The Kruger National Park claws were only sampled on the dorsal aspect of the unguis.

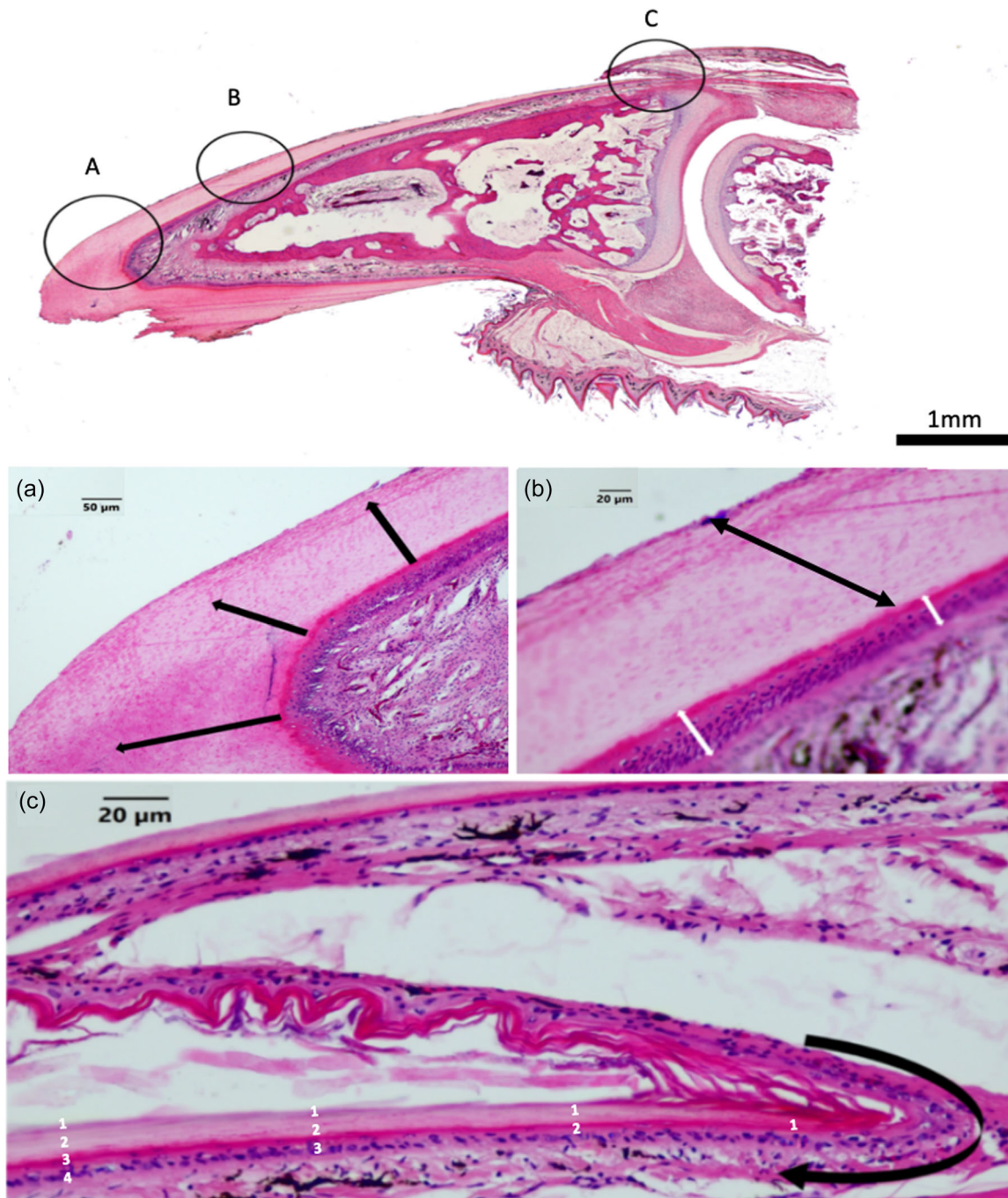


FIGURE 2 Histological sagittally sectioned claw from a hatchling Nile crocodile (H&E staining). Circled areas indicate the annotated magnified regions associated with images A, B, C. The black arrows in (a) and (b) indicate perpendicular cornification, and the white arrows demonstrate the region of mitotically active corneocytes. (c) Dorsal claw root angle (bent arrow) where claw growth in length and cornification is initiated. The white numbers illustrate the progressive corneal growth away from the root angle and away from the underlying basal epithelium. Thus, corneal matrix produced at white numbers: 1 (on the right), 2 (second from right), 3 (second from left), and 4 is of the same age. The age of the most superficial corneal matrix progressively increases towards the tip (distal) of the claw i.e., number 1 “on the right” is the earliest and number 1 “on the left” is the oldest. H&E, hematoxylin & eosin.

formed stacked layers that increase in thickness towards the apex (most distal region of the claw) where continual attrition wears down continually formed corneous material. In hatchlings, histological sections (Figures 2 and 3) investigating histomorphological characteristics of claw growth, showed that differentiating matrix/germ cells in the claw/“nail”

root (corneal angle) to specialized corneocytes, progressively cornifies from the base (proximally) towards the apex of the claw (distally). This results in the corneal layer produced at the base of the claw to be the thinnest and also the youngest, whereas the corneal layer at the apex is the thickest and the most dorsal (outer) layer in this region also the

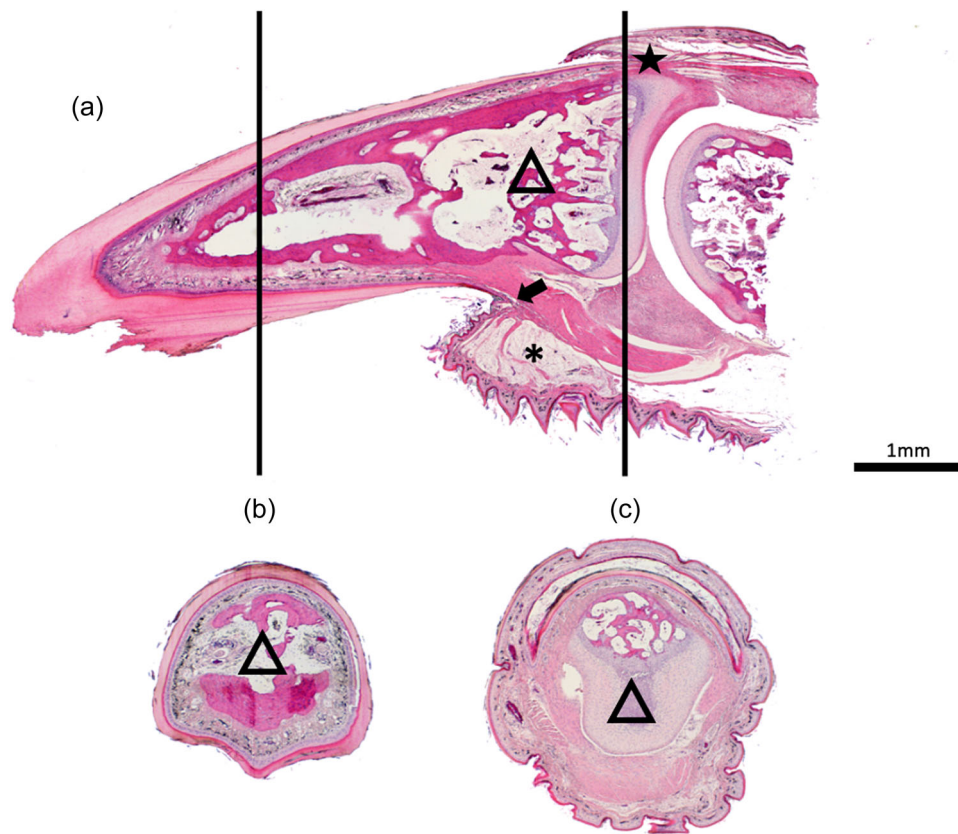


FIGURE 3 Histological sagittal (a) and transverse (b, c) sectioned claw from a hatchling Nile crocodile (H&E staining); (a) Dorsal—(star) and ventral (arrow) claw root angles. The ventral claw pad dermis comprises dense myxofibromatous tissue (asterisk). The black bars indicate the areas where transverse sections were made labeled as (b) and (c). (b) Transverse section through the distal third of the claw, demonstrating a uniformly cornified (light pink-stained outer eosinophilic layer) claw and a ventral sagittal ridge (black arrow). The distal phalanx bone forms the core of the claw (black triangle) (c) Transverse section through the dorsal and ventral claw root. H&E, hematoxylin & eosin.

oldest. Corneal growth is uniform around the distal phalanx (light pink-stained outer eosinophilic layer in Figure 3b) resulting in progressive thickening of the corneous matrix from the base (Figure 2c, white number: 1 to the right) towards the apex of the claw (Figure 2c, white number: 1 to the left). Ventrally, a specialized area reminiscent of a sole or “claw pad” is present (asterisk in Figure 3), characterized by deep epidermal folds at the ventral base of the claw overlying a localized area of dermal myxofibromatous (loose fibrous connective tissue embedded in a myxoid matrix) mesenchymal tissue. Dorsally, at the base of the claw, an acute angle (bent arrow in Figure 2c and arrow in Figure 3), formed in the distal hinge region of the last digital epidermal scute, contains the matrical cells from which corneal material producing corneocytes differentiates. The distal phalanx bone forms the core of the claw (black triangle in Figure 3).

Postmortem collected claws from Nile crocodiles larger than 3 m TL had layers of cornification that conformed to the growth pattern seen in hatchling crocodiles. This observation was fundamental to the use of claws as a proxy record (e.g., diet history reconstruction through stable light isotope analyses) for behavioral changes through time. It also provides the growth framework that can be calibrated in terms of age using radiocarbon dating. Since the ventral substrate contact region of the claw is most vulnerable to attrition, it stands to

reason that the less abraded surface on the most apical point of the dorsum of the claw would represent the oldest corneal matrix layer on the claw and thus the target area of radiocarbon dating.

Warthin-Starry stained histological sections of the corneal layers from adult crocodiles revealed clear stratification in the samples from the captive specimen, whereas discernable layering was much less apparent in the stratum corneum of the wild animal (Figure 4).

3.2 | Radiocarbon dating

A total of 20 radiocarbon dating analyses were made from seven claws ($n = 4$ each from the dorsal samples of claws from postmortem animals; $n = 4$ through the section of claw 3 and $n = 4$ from the scrapings of the claw tips of live animals), and the results are expressed with their associated errors in Table 1. Result that shows the presence of bomb carbon (i.e., results with >100 percent modern carbon [pMC]) must have formed since 1950). One result from Claw 3 fell within the range of the pre-1955 radiocarbon levels, but it is a relatively imprecise measurement, and the value is also within 2 standard deviations of the post-2020 radiocarbon levels. The shape of the bomb carbon curve further constrains the possible dates

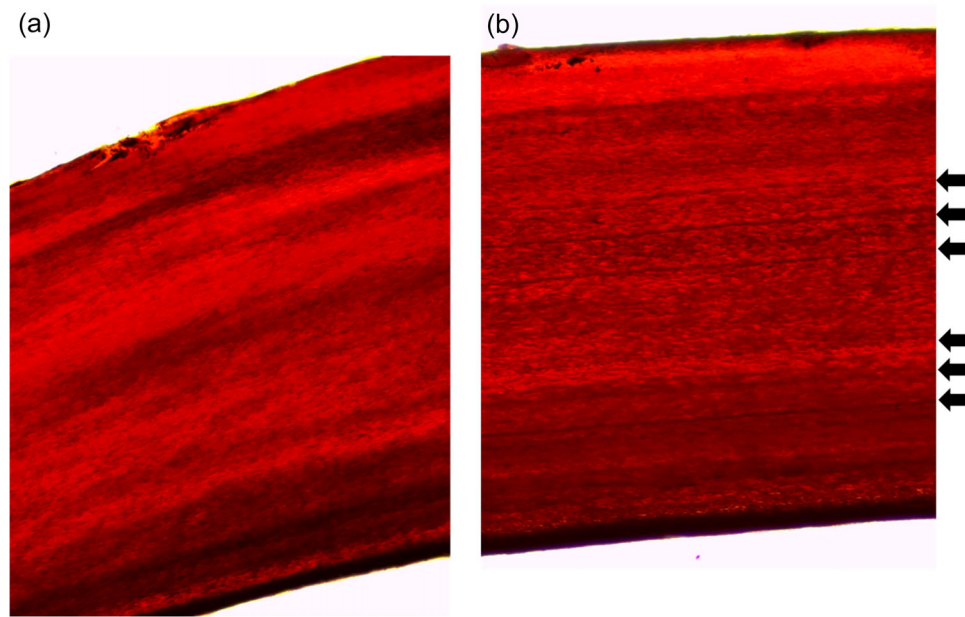


FIGURE 4 Warthin-Starry stained histological sections of the stratum corneum of the claws from an adult wild (a) and captive (b) crocodile. Note the well-defined corneal stratification in (b) where the darker lines (arrows) indicate periods of growth stagnation.

TABLE 1 Summary of radiocarbon results from Nile crocodile claws in the present study.

Sample/series ID	Position	pMC	pMC error
Claw a	Tip	103.36	0.34
Claw b	Tip	103.92	0.35
Claw c	Tip	102.99	0.35
Claw d	Tip	101.43	0.38
Claw 1	Tip	105.25	0.70
	Mid 1	105.36	0.71
	Mid 2	104.56	0.50
	Base	104.82	0.62
Claw 2	Tip	106.35	0.57
	Mid 1	105.74	0.60
	Mid 2	106.29	0.84
	Base	106.88	0.61
Claw 3 dorsal	Tip	102.30	1.38
	Mid 1	101.63	1.12
	Mid 2	104.77	1.07
	Base	104.39	0.53
Claw 3 section	Outer surface/tip	102.30	1.38
	Mid 1	98.27	0.90
	Mid 2	101.67	1.40
	Inner surface	102.27	1.90

Abbreviation: pMC, percent modern carbon.

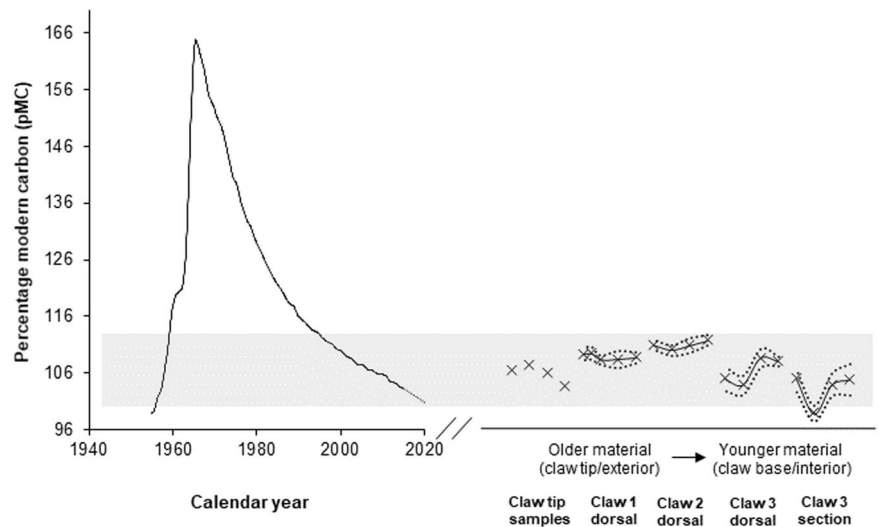
within the last 70 years. Tissue that formed between 1960 and 2000 will have radiocarbon values >110 pMC. The results from both dorsal/ventral, and longitudinal sample transects are all statistically <110 pMC at the 2-sigma level, and accordingly there is no evidence of claw tissue formed in the 1960–2000 period (Figure 5).

4 | DISCUSSION

4.1 | Histology

Histological evidence suggested that the growth of Nile crocodile claws led to an inherent age profile along two axes: one, along the dorsal surface of the unguis from the base to the apex (tip) of the claw, and another dorsoventrally through the corneal layer. As the epidermis grows distally following distally expanding phalangeal growth, cornification occurs continuously, resulting in the corneal layer directly adjacent to the basal epidermal cells to have the same age throughout the claw. Hence, the claw's very "outer" layer retains the oldest corneocytes for that specific segment. It can thus be concluded that the "outer/dorsal" region of the very "tip" (apex) of the claw would retain the oldest region of cornified material in a claw that was not subject to wear. This growth model coupled to similar patterns in the radiocarbon analyses of claw 3 through these two axes supports the growth patterns described here and elsewhere (Alibardi, 2021). The Warthin-Starry stained sections of the horny layers of adult crocodile claws supported the vertical growth pattern of the stratum corneum. As with most other horn producing species (Wang et al., 2016), differences in growth rates of the stratum corneum results in density differences of the deposited corneous material, which yields visible linear layers with

FIGURE 5 Radiocarbon values (expressed as pMC) of Nile crocodile claws compared with the atmospheric radiocarbon model of Turnbull et al. (2017) for the southern hemisphere zone 1–2. The shaded bar represents the area covered by the upper limits of the errors associated with one standard deviation. pMC, percent modern carbon.



the denser darker staining layers corresponding to periods of delayed/stagnant growth. These areas can thus be attributed to times of poor nutritional state and thus indicative of seasonality. In reptiles, these periods will also correspond to cold periods of the year where growth rate is retarded. In captivity, adult breeding crocodiles in non-artificially controlled environments (such as the animal used in the study) will not be fed much during winter, which results in very concise differences in growth rates, as opposed to wild crocodiles in temperate (natural) climates that may be feeding opportunistically and thus erratically throughout the year. Differences in growth rates in the latter group of animals is thus less concise, hence the lack of clearly discernable growth patterns in their claw corneal layers. Differences in chemical composition of the corneal matrix deposited determined by diet, season and growth rate are presumed to result in the layered appearance observed in the stratum corneum. Future studies focused on biochemical composition of the corneal layer is necessary to determine the true causality of the phenomenon.

4.2 | Radiocarbon dating

Radiocarbon dates revealed variable ages for the three claws. It was anticipated that older corneocytes would have higher pMC values as far back as about 1965 (corresponding to the peak in the bomb carbon curve), and so any cornified material that has formed in the last 70 years should reflect this peak (Hajdas et al., 2021; Taylor, 1997). None of the claws revealed any elevated radiocarbon associated with above-ground nuclear testing in the range 1960–1995. The radiocarbon dates therefore reveal variable ages from the claws of the large wild crocodiles, with Claw 2 producing the oldest age estimation and a calibrated cornification date of around 2010 (± 5 –10 years old). The absence of any evidence of corneous material produced in the 1960–1995 range in any of the samples suggests that it is doubtful that the Claw 3 result fell in the pre-1955 era, and the evidence indicated that all of the samples formed in the post 1995 era. All of the claws have estimated ages of <10 years (Figure 5).

The anticipated temporal trends from the dorsal/ventral and interior/exterior sample sequences of Claws 1, 2, and 3 were not noted, and there may be an indication of an inverted sequence, but the results reported in Table 1 show that all results from these transects are statistically indistinguishable from each other when the errors are considered. The lack of a trend suggests that wear and ongoing claw growth lead to a short temporal representation in the claw and that the notion of ageing Nile crocodiles by dating their claws was confounded by abrasion. Results from individual wild crocodile claws were consistent with the limited age noted in transects through and along the claws. These radiocarbon results suggest that there was little or no claw material that persisted for more than approximately 10 years in wild Nile crocodiles.

5 | CONCLUSION

It is almost certain that many of the crocodiles in this study were older than 10 years, and the issue becomes a balance between the growth of new cornified layers versus the rate at which abrasion removes older material from the claws. The cornified layers that are retained have an inherent age structure, but not reflective of the entire lifespan of the animal. The fish binge feeding hypothesis used by Woodborne et al. (2012) to explain “annual” $\delta^{15}\text{N}$ excursions along the unguis of Kruger National Park Nile crocodile claws may actually be a conflation of a progressively older signature moving distally from the base of the claw with a potentially progressively older sequence that results when wear exposes older corneocytes successively towards the tip of the claw in the area where the claw is thickest. Whether or not there is a duplication of the $\delta^{15}\text{N}$ pulses in a transect of the unguis does not affect the argument presented by Woodborne et al. (2012), as the overall number of pulses fall within the age range of claws, and they could conceivably reflect annual events. The evidence is consistent with the link between the river dynamics and the pansteatitis pandemics previously proposed. That the events are fish-eating binges cannot be unequivocally supported as self-metabolism (e.g., during starvation) is known to cause

increases in $\delta^{15}\text{N}$ values of animal tissues (Doi et al., 2017). However, limited research suggests that periods of fasting do not significantly affect the $\delta^{15}\text{N}$ values of reptilian claws (McCue & Pollock, 2008).

The methods described in Woodborne et al. (2012) for time series dietary reconstruction from crocodylian claws could be applied on living animals to infer trophic dynamics of the aquatic/terrestrial interface at a decadal scale (Santos et al., 2018; Woodborne et al., 2021). This has larger implications for managing the Nile crocodile population of the Olifants River Gorge in the Kruger National Park. Routine monitoring of the Olifants River Gorge system has persisted since 2011 with several complete aquatic food webs derived from stable isotope analyses since the onset of the first pansteatitis outbreak (Myburgh et al., 2022). Information is presently available to constrain the relationship between the $\delta^{15}\text{N}$ values of Nile crocodile claw time series and the trophic state of the food web in the Olifants River Gorge, and future studies should focus on providing a holistic picture of the dynamics of this ecosystem.

AUTHOR CONTRIBUTIONS

Albert Myburgh: Conceptualization; Methodology; Formal analysis; Writing—review & editing; Writing - original draft; Investigation; Validation. **Jan Myburgh:** Writing—review & editing; Investigation; Resources; Conceptualization. **Johan Steyl:** Methodology; Conceptualization; Visualization; Writing—original draft. **Colleen T. Downs:** Funding acquisition; Writing—review & editing; Project administration; Supervision. **Hannes Botha:** Investigation; Writing—review & editing; Writing - original draft; Data curation. **Liam Robinson:** Visualization; Writing—original draft; Formal analysis. **Stephan Woodborne:** Conceptualization; Methodology; Formal analysis; Investigation; Writing—review & editing; Supervision.

ACKNOWLEDGMENTS

We thank the IUCN Crocodile specialist group and the National Research Foundation (ZA) as well as IDEA Wild for providing funding that supported this research.

DATA AVAILABILITY STATEMENT

The data that support the findings of this study are available on request from the corresponding author. The data are not publicly available due to privacy or ethical restrictions.

ORCID

Albert Myburgh  <http://orcid.org/0000-0002-6891-1893>
 Jan Myburgh  <http://orcid.org/0000-0002-2132-7251>
 Johan Steyl  <http://orcid.org/0000-0002-5940-6799>
 Colleen T. Downs  <http://orcid.org/0000-0001-8334-1510>
 Hannes Botha  <https://orcid.org/0000-0001-6870-5494>
 Liam Robinson  <https://orcid.org/0000-0002-0549-7824>
 Stephan Woodborne  <https://orcid.org/0000-0001-8573-8626>

PEER REVIEW

The peer review history for this article is available at <https://www.webofscience.com/api/gateway/wos/peer-review/10.1002/jmor.21634>.

REFERENCES

- Alibardi, L. (1998). Differentiation of the epidermis during scale formation in embryos of lizard. *The Journal of Anatomy*, 192(2), 173–186. <https://doi.org/10.1046/j.1469-7580.1998.19220173.x>
- Alibardi, L. (2009). Development, comparative morphology and cornification of reptilian claws in relation to claws evolution in tetrapods. *Contributions to Zoology*, 78, 25–42. <https://doi.org/10.1163/18759866-07801003>
- Alibardi, L. (2010). Autoradiographic observations on developing and growing claws of reptiles. *Acta Zoologica*, 91, 233–241. <https://doi.org/10.1111/j.1463-6395.2009.00403.x>
- Alibardi, L. (2016). Sauropsids cornification is based on corneous beta-proteins, a special type of Keratin-associated corneous proteins of the epidermis: Keratinization and sauropsids cornification. *Journal of Experimental Zoology Part B: Molecular and Developmental Evolution*, 326B, 338–351. <https://doi.org/10.1002/jez.b.22689>
- Alibardi, L. (2021). Development, structure, and protein composition of reptilian claws and hypotheses of their evolution. *The Anatomical Record*, 304, 732–757. <https://doi.org/10.1002/ar.24515>
- Alibardi, L., & Thompson, M. B. (2002). Keratinization and ultrastructure of the epidermis of late embryonic stages in the alligator (*Alligator mississippiensis*). *Journal of Anatomy*, 201, 71–84. <https://doi.org/10.1046/j.1469-7580.2002.00075.x>
- Bancroft, J. D., & Gamble, M. (2002). Theory and practice of histological, *Techniques* (Fifth Edition). Churchill Livingstone. <https://doi.org/10.1111/j.1365-2559.1990.tb00755.x>
- Barquete, V., Strauss, V., & Ryan, P. G. (2013). Stable isotope turnover in blood and claws: A case study in captive African penguins. *Journal of Experimental Marine Biology and Ecology*, 448, 121–127. <https://doi.org/10.1016/j.jembe.2013.06.021>
- Boecklen, W. J., Yarnes, C. T., Cook, B. A., & James, A. C. (2011). On the use of stable isotopes in trophic ecology. *Annual Review of Ecology, Evolution, and Systematics*, 42, 411–440.
- Bowman, S. (1990). *Radiocarbon dating*. Vol. 1. Univ of California Press, Ca.
- Bronk Ramsey, C. (2008). Radiocarbon dating: Revolutions in understanding. *Archaeometry*, 50, 249–275. <https://doi.org/10.1111/j.1475-4754.2008.00394.x>
- Cerling, T. E., Wittemyer, G., Rasmussen, H. B., Vollrath, F., Cerling, C. E., Robinson, T. J., & Douglas-Hamilton, I. (2006). Stable isotopes in elephant hair document migration patterns and diet changes. *Proceedings of the National Academy of Sciences*, 103, 371–373. <https://doi.org/10.1073/pnas.0509606102>
- Chang, C., Wu, P., Baker, R. E., Maini, P. K., Alibardi, L., & Chuong, C. M. (2009). Reptile scale paradigm: Evo-Devo, pattern formation and regeneration. *The International Journal of Developmental Biology*, 53, 813–826. <https://doi.org/10.1387/ijdb.072556cc>
- Dalerum, F., & Angerbjörn, A. (2005). Resolving temporal variation in vertebrate diets using naturally occurring stable isotopes. *Oecologia*, 144, 647–658. <https://doi.org/10.1007/s00442-005-0118-0>
- Dawson, T. E., & Siegwolf, R. T. (2007). Using stable isotopes as indicators, tracers, and recorders of ecological change: Some context and background. *Terrestrial Ecology*, 1, 1–18. [https://doi.org/10.1016/s1936-7961\(07\)01001-9](https://doi.org/10.1016/s1936-7961(07)01001-9)
- Doi, H., Akamatsu, F., & González, A. L. (2017). Starvation effects on nitrogen and carbon stable isotopes of animals: An insight from meta-analysis of fasting experiments. *Royal Society Open Science*, 4, 170633. <https://doi.org/10.1098/rsos.170633>
- Dutta, K. (2016). Sun, ocean, nuclear bombs, and fossil fuels: Radiocarbon variations and implications for high-resolution dating. *Annual Review of Earth and Planetary Sciences*, 44, 239–275. <https://doi.org/10.1146/annurev-earth-060115-012333>
- Ethier, D. M., Kyle, C. J., Kyser, T. K., & Nocera, J. J. (2013). Trace elements in claw keratin as temporally explicit indicators of geographic origin in terrestrial mammals. *Annales Zoologici Fennici*, 50, 89–99. <https://doi.org/10.5735/086.050.0108>

- Ferreira, S. M., & Pienaar, D. (2011). Degradation of the crocodile population in the Olifants River gorge of Kruger National Park, South Africa. *Aquatic Conservation: Marine and Freshwater Ecosystems*, 21(2), 155–164. <https://doi.org/10.1002/aqc.1175>
- Hajdas, I., Ascough, P., Garnett, M. H., Fallon, S. J., Pearson, C. L., Quarta, G., Spalding, K. L., Yamaguchi, H., & Yoneda, M. (2021). Radiocarbon dating. *Nature Reviews Methods Primers*, 1, 62. <https://doi.org/10.1038/s43586-021-00058-7>
- Hobson, K. A. & Wassenaar, L. I., (Eds.). (2018). *Tracking animal migration with stable isotopes*. Academic Press.
- Hodge, E., McDonald, J., Fischer, M., Redwood, D., Hua, Q., Levchenko, V., Drysdale, R., Waring, C., & Fink, D. (2011). Using the 14 C bomb pulse to date young speleothems. *Radiocarbon*, 53, 345–357. <https://doi.org/10.1017/s0033822200056605>
- Hogg, A. G., Heaton, T. J., Hua, Q., Palmer, J. G., Turney, C. S., Southon, J., Bayliss, A., Blackwell, P. G., Boswijk, G., Bronk Ramsey, C., Pearson, C., Petchey, F., Reimer, P., Reimer, R., & Wacker, L. (2020). SHCal20 Southern hemisphere calibration, 0–55,000 years cal BP. *Radiocarbon*, 62(4), 759–778. <https://doi.org/10.1017/rdc.2020.59>
- Huchzermeyer, F. W. (2002). Diseases of farmed crocodiles and ostriches. *Revue Scientifique et Technique de l'OIE*, 21(1), 265–276. <https://doi.org/10.20506/rst.21.2.1334>
- Huchzermeyer, K. D. A. (2012). Prevalence of pansteatitis in African sharptooth catfish, *Clarias gariepinus* (Burchell), in the Kruger National Park, South Africa. *Journal of the South African Veterinary Association*, 83, 1–9. <https://doi.org/10.4102/jsava.v83i1.916>
- Krause, A., Sandmann, D., Bluhm, S. L., Ermilov, S., Widyastuti, R., Haneda, N. F., Scheu, S., & Maraun, M. (2019). Shift in trophic niches of soil microarthropods with conversion of tropical rainforest into plantations as indicated by stable isotopes (15N, 13C). *PLoS One*, 14, e0224520. <https://doi.org/10.1371/journal.pone.0224520>
- Layman, C. A., Araujo, M. S., Boucek, R., Hammerschlag-Peyer, C. M., Harrison, E., Jud, Z. R., Matich, P., Rosenblatt, A. E., Vaudo, J. J., Yeager, L. A., Post, D. M., & Bearhop, S. (2012). Applying stable isotopes to examine food-web structure: An overview of analytical tools. *Biological Reviews*, 87, 545–562. <https://doi.org/10.1111/j.1469-185x.2011.00208.x>
- Libby, W. F. (1954). Chicago radiocarbon dates V. *Science*, 120, 733–742. <https://doi.org/10.1126/science.120.3123.733>
- Maderson, P. F., & Alibardi, L. (2000). The development of the sauropsid integument: A contribution to the problem of the origin and evolution of feathers. *American Zoologist*, 40(4), 513–529. <https://doi.org/10.1093/icb/40.4.513>
- Mbele, V. L., Mullins, S. M., Winkler, S. R., & Woodborne, S. (2017). Acceptance tests for AMS radiocarbon measurements at iThemba LABS, Gauteng, South Africa. *Physics Procedia*, 90, 10–16. <https://doi.org/10.1016/j.phpro.2017.09.009>
- McCue, M. D., & Pollock, E. D. (2008). Stable isotopes may provide evidence for starvation in reptiles. *Rapid Communications in Mass Spectrometry*, 22, 2307–2314. <https://doi.org/10.1002/rcm.3615>
- Mülling, C. K. (2000). Three-dimensional appearance of bovine epidermal keratinocytes in different stages of differentiation revealed by cell maceration and scanning electron microscopic investigation. *Folia Morphologica*, 59, 239–246. <https://doi.org/10.5603/fm.2014.0039>
- Myburgh, A., Botha, H., Combrink, X., Myburgh, J., Guillette, Jr., L. J., Hall, G., Chimimba, C., & Woodborne, S. (2022). Terrestrial diet dependence in an unprotected Nile crocodile (*Crocodylus niloticus*) population. *Journal of Herpetology*, 56(4), 507–513. <https://doi.org/10.1670/21-060>
- Myburgh, J., & Botha, A. (2009). Decline in herons along the lower Olifants River—Could pansteatitis be a contributing factor. *Vet News*, 3, 20–23. <https://doi.org/10.4314/wsa.v37i1.64109>
- Nardoto, G. B., Sena-Souza, J. P., Chesson, L. A., & Martinelli, L. A. (2020). Tracking geographical patterns of contemporary human diet in Brazil using stable isotopes of nail corneus material. In R. C. Parra, S. C. Zapico & D. H. Ubelaker (Eds), *Forensic Science and Humanitarian Action: Interacting with the Dead and the Living*. Wiley (pp. 441–455). <https://doi.org/10.1002/9781119482062.ch28>
- Reimer, P. J., Brown, T. A., & Reimer, R. W. (2004). Discussion: Reporting and calibration of post-bomb 14C data. *Radiocarbon*, 46, 1299–1304. <https://doi.org/10.1017/s0033822200033154>
- Rutland, C. S., Cigler, P., & Kubale Dvojič, V. (2019). Reptilian skin and its special histological structures. In C. Rutland & V. Kubale (Eds), *Veterinary Anatomy and Physiology*. InTech. <https://doi.org/10.5772/intechopen.84212>
- Santos, X., Navarro, S., Campos, J. C., Sanpera, C., & Brito, J. C. (2018). Stable isotopes uncover trophic ecology of the West African crocodile (*Crocodylus suchus*). *Journal of Arid Environments*, 148, 6–13. <https://doi.org/10.1016/j.jaridenv.2017.09.008>
- Taylor, R. E. (1997). Radiocarbon dating. In R. E. Taylor & M. J. Aitken (Eds), *Chronometric dating in archaeology* (pp. 65–96). Springer https://doi.org/10.1007/978-1-4757-9694-0_3
- Tomlinson, D. J., Mülling, C. H., & Fakler, T. M. (2004). Invited review: Formation of keratins in the bovine claw: Roles of hormones, minerals, and vitamins in functional claw integrity. *Journal of Dairy Science*, 87, 797–809. [https://doi.org/10.3168/jds.s0022-0302\(04\)73223-3](https://doi.org/10.3168/jds.s0022-0302(04)73223-3)
- Turnbull, J. C., Mikaloff Fletcher, S. E., Ansell, I., Brailsford, G. W., Moss, R. C., Norris, M. W., & Steinkamp, K. (2017). Sixty years of radiocarbon dioxide measurements at Wellington, New Zealand: 1954–2014. *Atmospheric Chemistry and Physics*, 17, 14771–14784. <https://doi.org/10.5194/acp-17-14771-2017>
- Wang, B., Yang, W., McKittrick, J., & Meyers, M. A. (2016). Keratin: Structure, mechanical properties, occurrence in biological organisms, and efforts at bioinspiration. *Progress in Materials Science*, 76, 229–318. <https://doi.org/10.1016/j.pmatsci.2015.06.001>
- Wang, Y., Gu, B., Lee, M. K., Jiang, S., & Xu, Y. (2014). Isotopic evidence for anthropogenic impacts on aquatic food web dynamics and mercury cycling in a subtropical wetland ecosystem in the US. *Science of the Total Environment*, 487, 557–564. <https://doi.org/10.1016/j.scitotenv.2014.04.060>
- Woodborne, S., Botha, H., Huchzermeyer, D., Myburgh, J., Hall, G., & Myburgh, A. (2021). Ontogenetic dependence of Nile crocodile (*Crocodylus niloticus*) isotope diet-to-tissue discrimination factors. *Rapid Communications in Mass Spectrometry*, 35, e9159. <https://doi.org/10.1002/rcm.9159>
- Woodborne, S., Huchzermeyer, K. D. A., Govender, D., Pienaar, D. J., Hall, G., Myburgh, J. G., Deacon, A. R., Venter, J., & Lübcker, N. (2012). Ecosystem change and the Olifants River crocodile mass mortality events. *Ecosphere*, 3(10), art87. <https://doi.org/10.1890/es12-00170.1>
- Vander Zanden, M. J., Casselman, J. M., & Rasmussen, J. B. (1999). Stable isotope evidence for the food web consequences of species invasions in lakes. *Nature*, 401, 464–467. <https://doi.org/10.1038/46762>

How to cite this article: Myburgh, A., Myburgh, J., Steyl, J., Downs, C. T., Botha, H., Robinson, L., & Woodborne, S. (2023). The histology and growth rate of Nile crocodile (*Crocodylus niloticus*) claws. *Journal of Morphology*, 284, e21634. <https://doi.org/10.1002/jmor.21634>